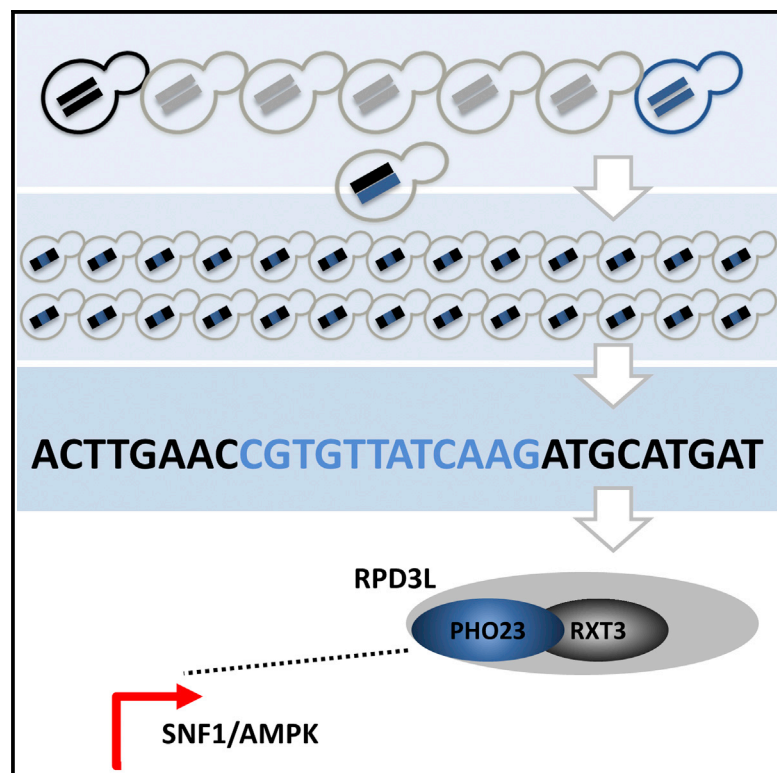


Cell Reports

Natural Diversity in Pentose Fermentation Is Explained by Variations in Histone Deacetylases

Graphical Abstract



Authors

Zvi Tamari, Naama Barkai

Correspondence

naama.barkai@weizmann.ac.il

In Brief

Tamari and Barkai performed a quantitative trait loci study on ethanol production from the pentose sugar xylulose in budding yeast. Variations in components of the large Rpd3 histone deacetylation complex are causal to increased ethanol production. These variants modulate expression of SNF1/AMPK-dependent respiratory genes.

Highlights

- Natural strains of budding yeast show variable xylulose fermentation
- Causal alleles are mapped to components of RPD3L histone deacetylase complex
- Alleles of this complex differentially modulate respiratory genes' expression

Accession Numbers

GSE75673



Natural Diversity in Pentose Fermentation Is Explained by Variations in Histone Deacetylases

Zvi Tamari^{1,2} and Naama Barkai^{1,*}

¹Department of Molecular Genetics, Weizmann Institute of Science, Rehovot 76100, Israel

²Present address: Department of Chemical and Biomolecular Engineering, University of California, Los Angeles, Los Angeles, CA 90095, USA

*Correspondence: naama.barkai@weizmann.ac.il

<http://dx.doi.org/10.1016/j.celrep.2015.12.048>

This is an open access article under the CC BY-NC-ND license (<http://creativecommons.org/licenses/by-nc-nd/4.0/>).

SUMMARY

The extent to which carbon flux is directed toward fermentation versus respiration differs between cell types and environmental conditions. Understanding the basic cellular processes governing carbon flux is challenged by the complexity of the metabolic and regulatory networks. To reveal the genetic basis for natural diversity in channeling carbon flux, we applied quantitative trait loci analysis by phenotyping and genotyping hundreds of individual F2 segregants of budding yeast that differ in their capacity to ferment the pentose sugar xylulose. Causal alleles were mapped to the RXT3 and PHO23 genes, two components of the large Rpd3 histone deacetylation complex. We show that these allelic variants modulate the expression of SNF1/AMPK-dependent respiratory genes. Our results suggest that over close evolutionary distances, diversification of carbon flow is driven by changes in global regulators, rather than adaptation of specific metabolic nodes. Such regulators may improve the ability to direct metabolic fluxes for biotechnological applications.

INTRODUCTION

The budding yeast *Saccharomyces cerevisiae* is unique in its exceptional capacity to ferment sugar even in the presence of oxygen, a phenomenon known as the Crabtree effect. This effect is most pronounced during growth on glucose, although high levels of ethanol production also are observed during growth on other related carbon sources, such as fructose and galactose. However, in the presence of sub-optimal carbon sources, the distribution of carbon flux among ethanol, biomass accumulation, and complete oxidation to CO₂ can vary considerably (Gancedo, 1998; Polakis and Bartley, 1965). Accordingly, a complex network of signaling pathways that orchestrates the channeling of carbon flux in response to changes in environmental conditions was characterized (Johnston and Marian, 1992).

Production of ethanol by fermentation of lignocellulose, the most abundant organic matter on Earth, is an attractive alterna-

tive to petroleum-based fuels (Service, 2014). While lignocellulose is comprised of both hexose (primarily glucose) and pentose (primarily xylose) sugars, budding yeast can naturally ferment only the hexose portion. There is, therefore, a great interest in understanding how to rewire central carbon metabolism to allow for increasing (and sometimes decreasing) ethanol production when growing on any given carbon source. While this is typically explored by a genetic engineering approach, natural diversity between related strains can be informative on how such rewiring is achieved during the course of evolution. We recently reported that natural strains of *S. cerevisiae* differ greatly in their ability to ferment xylulose, the only pentose yeast that can naturally metabolize (Tamari et al., 2014). We therefore used this system as a model to identify the genetic variants that contribute to this natural diversity in pentose fermentation.

RESULTS AND DISCUSSION

Among a collection of 12 wild-type *S. cerevisiae* isolates originating from diverse geographical origins and natural habitats (Table S1), T73 and Y12 produced the most ethanol, while CLIB215 produced the least amounts of ethanol, although growing at comparative rates (Figures 1A and 1B). T73 showed increased ethanol production rate and, therefore, was selected, together with CLIB215, for further analysis. In contrast to phenotypic diversity observed in xylulose fermentation, all strains produced approximately the same ethanol levels when grown on glucose (Tamari et al., 2014).

We used quantitative trait locus (QTL) analysis to define genetic variants associated with this difference in xylulose fermentation. T73 and CLIB215 were crossed, sporulated, and over a thousand F2 segregants were phenotyped for ethanol production and growth on xylulose ($n = 1,061$) (Figure 1C). Significant diversity was observed among segregants, including a 1% transgressive segregation rate (Figure 1D). No correlation was observed between the amount of ethanol produced and optical density reached at saturation, suggesting that differences in ethanol production resulted from differential carbon distribution between fermentation and respiration, rather than differences in biomass production.

We selected the 150 segregants producing the highest amounts of ethanol and the 150 segregants producing the lowest amounts of ethanol and genotyped them individually using restriction site-associated DNA sequencing (Baird et al., 2008;

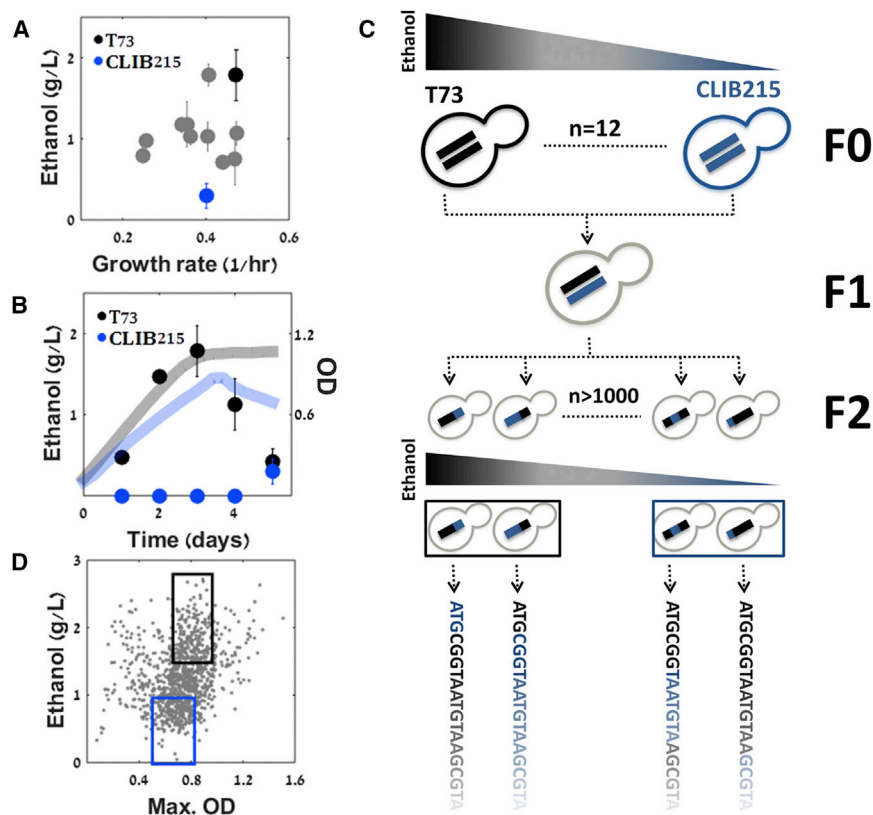


Figure 1. F0 and F2 Selection and Workflow Scheme

(A) Growth rates versus ethanol production of 12 wild-type *S. cerevisiae* strains grown on xylulose (n = 8 repeats), including the two selected extreme strains, T73 (black) and CLIB215 (blue). See also Table S1.

(B) Time course measurements of ethanol production (circles, left axis) and OD levels (shaded lines, right axis) during growth on xylulose for 5 days of the two selected strains are shown (n = 8 repeats).

(C) QTL analysis workflow for natural divergence in ethanol production. Wild-type *S. cerevisiae* strains (12) were phenotyped for their ethanol production from xylulose. The two extreme strains were selected as the F0 generation. These strains were crossed, the resulting hybrid was sporulated, and several individual F2 segregants (n = 1,061) were isolated. The segregants were phenotyped for ethanol production from xylulose and two extreme groups, comprised of 150 segregants each, were selected. The genome of each of the 300 extreme segregants was sequenced for further QTL analysis.

(D) Maximum OD levels reached during growth on xylulose versus ethanol production levels of each F2 segregant. The 150 extreme high ethanol-producing segregants (black box) and 150 low ethanol-producing segregants (blue box) were selected for further analysis.

Figure S1). Altogether, we identified ~42,500 sequence variants, which enabled the definition of parental allele frequency in each chromosomal position (Figure 2A). Significance of association of specific parental alleles with the efficiency of ethanol production was tested and the false discovery rate was controlled using the Bonferroni method, from which the LOD score for co-segregation was obtained.

Seven QTLs co-segregated with increased ethanol production (Figure 2B). In four of them, including the two with highest LOD scores, increased ethanol production was linked to the allele of the high ethanol-producing parent, T73. Notably, one of these QTLs (chromosome 7) includes the *XKS1* gene, which performs the first enzymatic reaction for introducing xylulose into central carbon metabolism (phosphorylation of xylulose to the pentose-phosphate pathway intermediate xylulose-5-P). In the three remaining loci, the low ethanol-producing parent CLIB215 allele was associated with increased ethanol production, reminiscent of the observed transgressive segregation in ethanol measurements of the F2 progeny.

Four QTLs (chromosomes 4, 7, 9, and 14) were confined to relatively short chromosomal regions (~3 kb). To begin verifying their effects, we swapped these regions between the two parent strains, replacing the predicted low-producing alleles with the high-producing ones (Figure 3A). Introducing the predicted T73 regions from chromosomes 4 and 7 into CLIB215 increased ethanol production by 6.5-fold and 4.3-fold, respectively (Figure 3B), thus validating their causal effects. In contrast, allelic replacement of the predicted high-variant QTLs in chromosomes

9 and 14 from CLIB215 to T73 did not increase ethanol production significantly (Figure S2), possibly due to their low effect, inaccurate positioning of the QTLs, or a mechanism involving epistatic interactions.

Each of the identified QTLs included several genes. To identify the individual gene(s) causal for the QTL effect, candidate genes were selected from broad regions spanning the peak center.

These genes were chosen by identifying a non-synonymous sequence variation in the open reading frame (ORF); a sequence variation in the 5'-UTR, 3'-UTR, proximal transcription-related protein-binding site; or TATA-like element (Venters et al., 2011; Nagalakshmi et al., 2008; Rhee and Pugh, 2012). In total, 38 candidate genes taken from six QTL regions were selected (Table S2). Allelic replacement was performed on a BY4741 background as follows: for each candidate gene, the BY4741 allele was replaced by either the T73 or the CLIB215 allele and ethanol production from xylulose was quantified.

A significant difference in ethanol production between the T73 and CLIB215 alleles was observed in five genes (Figure 3C). For two of these genes, *RXT3* (chromosome 4) and *PHO23* (chromosome 14), the difference was associated with increased ethanol production above that of the wild-type BY4741 background. The sequence variations associated with these genes included two non-synonymous mutations in *RXT3* (Figure 3D) and five mutations in binding sites of transcription-related proteins in the *PHO23* promoter region (Figure 3E). In the three remaining genes, *SAL1*, *EAF3*, and *YME1*, differential ethanol production was a result of reduced ethanol production by the low-allele

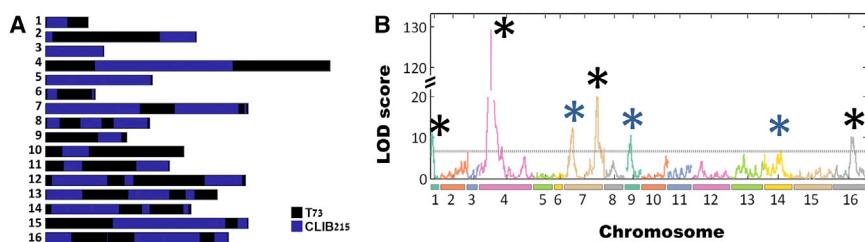


Figure 2. Identification of QTL

(A) Complete set of chromosomal maps of a representative segregant. Such maps were constructed for each of the 300 sequenced segregants.

(B) LOD score ($-\log(p.v.)$) for randomly observing the given allelic distribution between the high and low parents per position, across the whole genome. Peaks (QTLs) marked with black asterisks correspond to loci in which the high ethanol parent allele was as-

sociated with increased segregant ethanol production, while QTLs marked with blue asterisks correspond to loci in which the low ethanol parent allele linked with increased ethanol production. Dashed line marks the Bonferroni cutoff level. See also Figure S1.

strain, below the amounts produced by the wild-type BY4741 background.

Interestingly, RXT3 and PHO23 are both components of the large Rpd3 histone deacetylase complex (HDAC) (Carrozza et al., 2005a). Furthermore, EAF3 also is associated with Rpd3 HDAC, but with the small complex (Carrozza et al., 2005b). Consistent with QTL allelic association, a BY4741 strain containing the T73 *RXT3* allele produced more ethanol compared to the strain containing the CLIB215 allele. The opposite was true for the two *PHO23* alleles, consistent with its predicted association. Notably, *PHO23* was not included in the 2.5-kb region used during allele swapping between CLIB215 and T73, possibly explaining the lack of ethanol induction following the large-scale QTL allelic replacement. An additional effect was observed by replacing the native *XKS1* allele of BY4741 by either the T73 or CLIB215 allele, which dramatically reduced the amount of ethanol produced in both cases. This reduction might be explained by the interruption of the regulatory region by the selection marker. We did not follow up on this observation but rather focused on the effect of the Rpd3 genes showing the largest effects.

Rpd3 previously was identified as a general repressor of gene expression, regulating the expression of a large number of genes (Vidal and Gaber, 1991; Vidal et al., 1991; Kuo and Allis, 1998). Recruitment to specific genes depends on co-repressors, such as UME6 (Kadosh and Struhl, 1997). The Rpd3 HDAC also is responsible for the constitutive low level of acetylation of a large fraction of the genome (Weinberger et al., 2012). The induction of ethanol production by Rpd3 genes, therefore, may be due to changes in the transcriptional program. To examine this, we profiled gene expression of *RXT3* and *PHO23* allelic replacement strains (BY4741^{T73-RXT3}, BY4741^{CLIB215-RXT3}, BY4741^{T73-PHO23}, and BY4741^{CLIB215-PHO23}), as well as the respective deletion strains (BY4741^{ΔRXT3} and BY4741^{ΔPHO23}), during growth on xylulose.

In yeast, carbon utilization is tightly regulated at the level of gene transcription (Zaman et al., 2008). Glucose, for example, represses genes required for respiration and genes involved in alternative carbon metabolism. This repression depends on several signaling pathways, including Ras/PKA, Rgt, and Snf1, which affect partially overlapping sets of genes (Santangelo, 2006). In all our strains, including the high and low ethanol-producing allele strains, growth on xylulose de-repressed most of the glucose-repressed genes, and their expression remained largely similar. A notable exception was the set of genes normally induced in the presence of an alternative carbon source via the

SNF1-dependent pathway (Zaman et al., 2009). Expression of these genes was significantly lower in the high ethanol-producing strains BY4741^{T73-RXT3} and BY4741^{CLIB215-PHO23} (p values = 10^{-5} and $10^{-4.5}$, respectively; Figure 4). Closer examination revealed that differential expression was associated with the CAT8-dependent branch of this pathway (p values = 10^{-5} and 10^{-8} for BY4741^{T73-RXT3} and BY4741^{CLIB215-PHO23}, respectively) and not with the ADR1 branch (p value > 0.05 for both BY4741^{T73-RXT3} and BY4741^{CLIB215-PHO23}). Indeed, CAT8 is known to activate respiratory metabolism under SNF1-regulated conditions (Tachibana et al., 2005; Young et al., 2003), while CAT8 deletion was shown to increase ethanol production, even when cells are grown on glucose, by downregulating the expression of genes associated with respiration (Qi et al., 2014; Watanabe et al., 2013). Furthermore, a role of histone acetylation in activation of CAT8-regulated genes was described previously (Abate et al., 2012). Together, our results suggest that differential xylulose fermentation might result from distinct activation levels of the CAT8 branch of the SNF1-signaling pathway by the different Rpd3 HDAC variants.

Understanding the regulatory elements that direct carbon flux toward fermentation in yeast is important from both scientific and biotechnological perspectives, as it is essential for achieving efficient cellulosic ethanol production. In this study, we identified components of the HDAC Rpd3L that can facilitate ethanol production from xylulose. Our finding that in nature initial adaptation of metabolic flux is achieved by mutations in general regulatory factors may suggest that tuning such factors may be beneficial when attempting to engineer yeast strains for biotechnological applications.

EXPERIMENTAL PROCEDURES

Strain Collection

S. cerevisiae strains YPS1009, T7, T73, PW5, Y12, CLIB324, CLIB215, CBS7960, and YJM269 were a kind gift from Dr. Justin Fay, Genome Institute, Washington University. *S. cerevisiae* strain EC1118 was purchased from Micha Lerer.

Xylulose Production

Mixtures of xylulose and xylose were produced in the lab following the method described previously (Olsson et al., 1994). Xylose (350 g, Sigma-Aldrich) was dissolved in 500 ml water and 20 g immobilized Xylose Isomerase (Sigma-Aldrich) was added. This mixture was incubated at 60°C for 24 hr with agitation (300 rpm). The enzyme was inactivated by heating to 100°C and then filtered off. The resulting xylose:xylulose ratio was determined by high-performance liquid chromatography (HPLC) analysis.

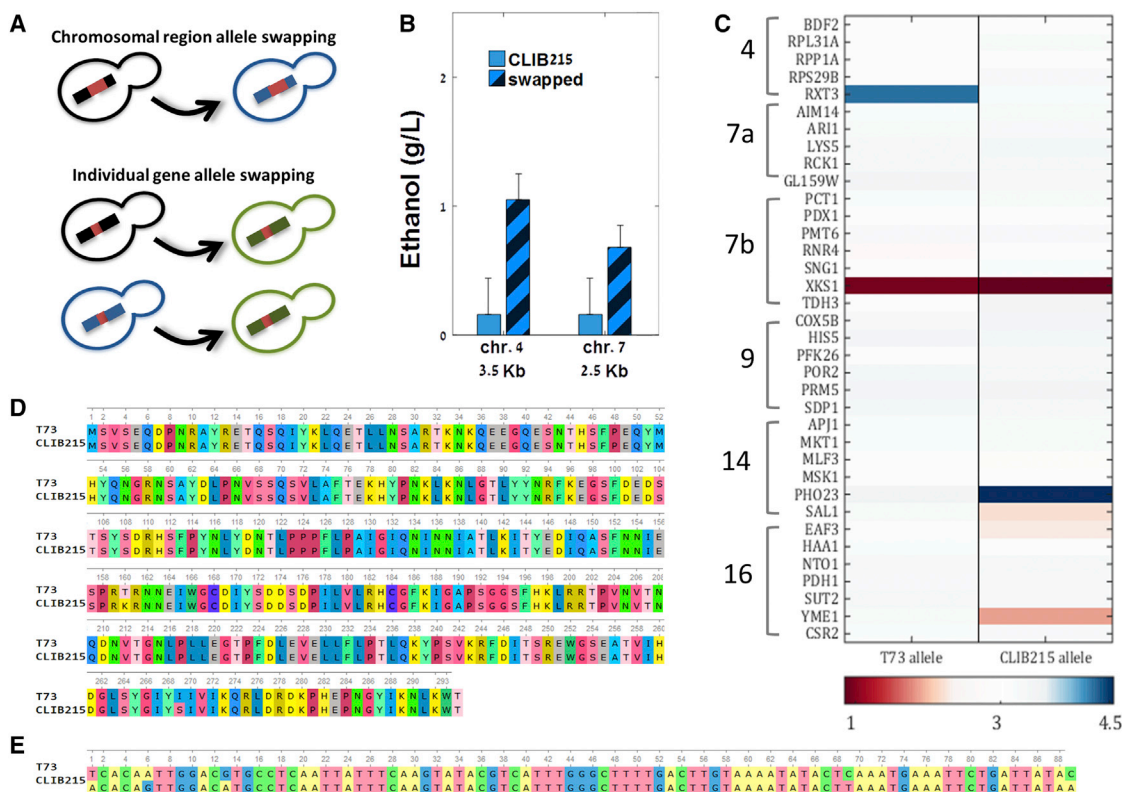


Figure 3. QTL Dissection

(A) Two methods of QTL dissection were implemented. First, chromosomal regions confined inside the QTL boundaries were swapped by replacing the low ethanol-producing parent (blue cartoon) CLIB215 region with that of the high ethanol-producing parent (black cartoon) T73 region (top). Second, individual gene causal effects were tested by replacing the BY4741 (green cartoon) allele with that of T73 and CLIB215 and comparing ethanol production of the two resulting strains (bottom). This was performed for each of the tested genes.

(B) Ethanol production of CLIB215 versus swapped strains, for chromosomes 4 and 7 QTL region swapping, as described in the top part of (A). The lengths of the chromosomal regions that were swapped are indicated. See also [Figure S2](#).

(C) Ethanol production comparison between T73 and CLIB215 alleles of 38 genes from the identified QTLs, divided according to chromosomes (two QTLs were mapped to chromosome 7). The alleles were introduced into the same genetic background (BY4741), replacing the native allele, as described in the bottom part of (A). See also [Table S2](#).

(D) RXT3 alignment of T73 and CLIB215 alleles shows the two identified non-synonymous mutations (positions 160 and 269).

(E) Alignment shows the PHO23 regulatory region containing five sequence variations in transcription-related protein-binding sites.

Metabolite Concentration Measurements

The concentrations of xylulose, glycerol, and ethanol were measured using an Agilent 1200 series HPLC system equipped with an anion exchange Bio-Rad HPX-87H column. When sugar concentrations were measured, a long column was used (300 × 7.8 mm). The column was eluted with 5 mM sulfuric acid at a flow rate of 0.6 ml/min at 45°C. For high-throughput ethanol measurements, a short Fast Acid Analysis column was used (100 × 7.8 mm). The column was eluted with 5 mM sulfuric acid at a flow rate of 1 ml/min at 45°C. All measurements were performed in 96-well plates. Sample filtering for HPLC analysis was performed by mounting AcroPrep™ Advanced Filter Plates (Pall) on 96-well plates and centrifugation. To minimize ethanol evaporation during runtime, plates were sealed with 96-well plate pierceable closing mats (Thermo Scientific).

Yeast Growth Experiments

For wild-type yeast strain growth rate measurement on xylulose, strains were grown in 50-ml starter tubes for 2 days in 5 ml YP-xylulose + xylose (2% xylulose) and then diluted to optical density (OD) 0.1 in 5 ml YP-xylulose + xylose (2% xylulose). OD measurements were taken every 30 min and doubling times were calculated by plotting log₂ OD levels versus time.

F2 segregant growth was conducted using a Tecan Evolution200 robot. Cells were pre-grown on rich media (YP-xylulose + xylose, 2% xylulose) for

2 days and then inoculated to a starting OD of 0.1 into 96-well plates containing 150 μl YP-xylose + xylulose. Mineral oil (30 μl) was added to each well to eliminate evaporation. Plates were incubated in 30°C in a robotic incubator with gentle agitation. OD measurements were taken every 30 min following a 1-min strong agitation period (1,400 rpm) prior to each measurement.

F2 Generation

The HO locus of wild-type T73 and CLIB215 strains was replaced with either Kanamycin or Nourseothricin. T73 (HO::Kanamycin) and CLIB215 (HO::Nourseothricin) strains were mated. The resulting hybrid was sporulated using standard presporulation medium/sporulation medium (SPS/SPM) sporulation protocol. Segregant single colonies (1,350) were individually picked and transferred to 96-well plates. To verify that segregants were haploid, each segregant was grown on YPD + Kanamycin and on YPD + Nourseothricin and only segregants that grew on one selection media and not on the other were chosen for further analysis.

DNA and RNA Sequencing

Genomic DNA from 300 *S. cerevisiae* F2 segregants, the two F0 wild-type strains T73 and CLIB215, and their hybrid was individually extracted using the Yeast Genomic DNA 96-Well Isolation Kit (Norgen Biotek). DNA

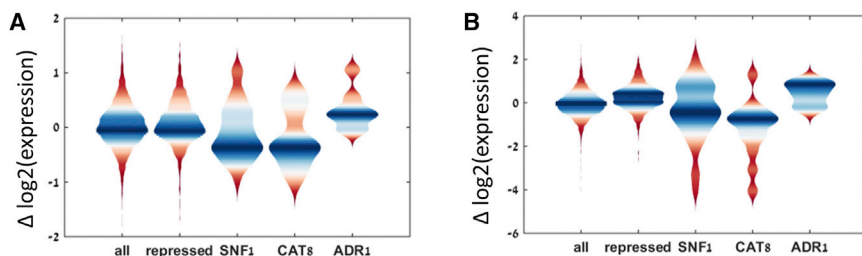


Figure 4. Expression Effect of Causal Genes

Distribution of expression level (\log_2) difference between high and low ethanol production allelic replacement strains of *RXT3* (BY4741^{T73-RXT3}/BY4741^{CLIB215-RXT3}) (A) and *PHO23* (BY4741^{CLIB215-PHO23}/BY4741^{T73-PHO23}) (B) for different gene groups during growth on xylulose. Gene groups include all annotated genes in *S. cerevisiae* (all), glucose-repressed genes (repressed), SNF1-regulated genes (SNF1), and the subset of SNF1-regulated genes associated with either CAT8 (CAT8) or ADR1 (ADR1). Results are the mean of three RNA sequencing repeats.

concentrations were measured using PicoGreen double-stranded DNA (dsDNA) quantitation kit (Life Technologies) and measured in a fluorescent plate reader.

DNA RADSeq sequencing was performed by Texas A&M Agrilife Research using an Illumina HiSeq2000 platform with 100-bp paired-ends reads. Raw data analysis was carried out using FastQC v0.10.1 (Babraham Institute) and FASTX-trimmer. Read data were aligned to the *S. cerevisiae* S288c reference genome (SGD R64) using Burrows-Wheeler Aligner (BWA). The GATK toolkit (Broad Institute) was used for local realignment around indels, base quality score recalibration, and SNP calling.

For RNA sequencing, log-phase cells were harvested and frozen in liquid nitrogen. Total RNA was extracted using a NucleoSpin 96 RNA kit (Macherey-Nagel), substituting β -mercaptoethanol with DTT. cDNA was barcoded and sequencing was performed using Illumina HiSeq2500 platform with 50-bp single reads. Reads were mapped to the *S. cerevisiae* S288c reference genome (SGD R64) using Bowtie. Reads mapping to rRNA were filtered out. Normalization for PCR bias was carried out using unique molecular identifier (UMI) scoring (Kivioja et al., 2011). Per-strain mapped reads were normalized to 106 and per-gene mapped reads were normalized by the total number of reads across all sequenced strains.

Functional Analysis of Gene Expression Changes

For expression analysis of glucose-repressed genes, genes were defined using the expression dataset in Gasch et al. (2000) and choosing those genes whose expression level was downregulated at least twice in stationary phase compared to log phase.

Identification of functional gene groups whose expression was significantly altered between high and low ethanol allele strains was achieved by first defining the set of genes representing the most significant changes, followed by enrichment analysis by projecting these gene groups on pre-defined functional gene groups (Ihmels et al., 2002). To determine the significance of expression changes associated with CAT8 versus ADR1 branches, a hypergeometric test was used based on functional gene data in Zaman et al. (2009).

Chromosomal Region Swapping and Individual Gene Allelic Replacement

For chromosomal region swapping, a Hygromycin (Hyg) resistance marker was introduced adjacent to the chromosomal region of the high ethanol-producing parent. Hyg-containing loci from the high ethanol-producing parent were subject to PCR and introduced into the low ethanol-producing parent, replacing the native locus by homologous recombination. Single-colony transformants were then selected from YPD-Hyg agar plates.

For allelic replacement experiments, each gene was first deleted in BY4741 using a Kanamycin selection marker. T73 and CLIB215 alleles of each gene were cloned into a pYM-N14 plasmid downstream of a Hyg resistance marker. Gene regulatory regions also were included by taking the 500 bp upstream of the 5'-end of the ORF and the 100 bp downstream of the 3'-end of the ORF, unless another gene was found in these limits, in which case the regulatory region was defined up until the adjacent gene. Finally, the allele + Hyg resistance

gene was introduced into the deletion strains, replacing the Kanamycin resistance marker.

ACCESSION NUMBERS

The accession number for the RNA sequencing data reported in this paper is GEO: GSE75673. The Entrez Sequence Read Archive accession number for the RAD-seq data is SRP067672.

SUPPLEMENTAL INFORMATION

Supplemental Information includes two figures and two tables and can be found with this article online at <http://dx.doi.org/10.1016/j.celrep.2015.12.048>.

AUTHOR CONTRIBUTIONS

Z.T. and N.B. designed the experiments, analyzed results, and wrote the paper. Z.T. conducted the experiments.

ACKNOWLEDGMENTS

This work was supported by the Israel Science Foundation, The European Research Council, and The Israeli Ministry of Science and Technology.

Received: June 22, 2015

Revised: September 13, 2015

Accepted: December 7, 2015

Published: January 7, 2016

REFERENCES

- Abate, G., Bastonini, E., Braun, K.A., Verdone, L., Young, E.T., and Caserta, M. (2012). Snf1/AMPK regulates Gcn5 occupancy, H3 acetylation and chromatin remodelling at *S. cerevisiae* ADY2 promoter. *Biochim. Biophys. Acta* 1819, 419–427.
- Baird, N.A., Etter, P.D., Atwood, T.S., Currey, M.C., Shiver, A.L., Lewis, Z.A., Selker, E.U., Cresko, W.A., and Johnson, E.A. (2008). Rapid SNP discovery and genetic mapping using sequenced RAD markers. *PLoS ONE* 3, e3376.
- Carrozza, M.J., Florens, L., Swanson, S.K., Shia, W.J., Anderson, S., Yates, J., Washburn, M.P., and Workman, J.L. (2005a). Stable incorporation of sequence specific repressors Ash1 and Ume6 into the Rpd3L complex. *Biochim. Biophys. Acta* 1731, 77–87.
- Carrozza, M.J., Li, B., Florens, L., Sugauma, T., Swanson, S.K., Lee, K.K., Shia, W.J., Anderson, S., Yates, J., Washburn, M.P., and Workman, J.L. (2005b). Histone H3 methylation by Set2 directs deacetylation of coding regions by Rpd3S to suppress spurious intragenic transcription. *Cell* 123, 581–592.
- Gancedo, J.M. (1998). Yeast carbon catabolite repression. *Microbiol. Mol. Biol. Rev.* 62, 334–361.

- Gasch, A.P., Spellman, P.T., Kao, C.M., Carmel-Harel, O., Eisen, M.B., Storz, G., Botstein, D., and Brown, P.O. (2000). Genomic expression programs in the response of yeast cells to environmental changes. *Mol. Biol. Cell* **11**, 4241–4257.
- Ihmels, J., Friedlander, G., Bergmann, S., Sarig, O., Ziv, Y., and Barkai, N. (2002). Revealing modular organization in the yeast transcriptional network. *Nat. Genet.* **31**, 370–377.
- Johnston, M., and Marian, C. (1992). Carbon regulation in *Saccharomyces*. In *The Molecular Biology of the Yeast Saccharomyces: Gene Expression*, J.B.E.W. Jones and J.R. Pringle, eds. (Cold Spring Harbor, NY: Cold Spring Harbor Lab. Press), pp. 198–281.
- Kadosh, D., and Struhl, K. (1997). Repression by Ume6 involves recruitment of a complex containing Sin3 corepressor and Rpd3 histone deacetylase to target promoters. *Cell* **89**, 365–371.
- Kivioja, T., Vähärautio, A., Karlsson, K., Bonke, M., Enge, M., Linnarsson, S., and Taipale, J. (2011). Counting absolute numbers of molecules using unique molecular identifiers. *Nat. Methods* **9**, 72–74.
- Kuo, M.H., and Allis, C.D. (1998). Roles of histone acetyltransferases and deacetylases in gene regulation. *Bioessays* **20**, 615–626.
- Nagalakshmi, U., Wang, Z., Waern, K., Shou, C., Raha, D., Gerstein, M., and Snyder, M. (2008). The transcriptional landscape of the yeast genome defined by RNA sequencing. *Science* **320**, 1344–1349.
- Olsson, L., Lindén, T., and Hahn-Hägerdal, B. (1994). A rapid chromatographic method for the production of preparative amounts of xylulose. *Enzyme Microb. Technol.* **16**, 388–394. <http://www.sciencedirect.com/science/article/pii/0141022994901538>.
- Polakis, E.S., and Bartley, W. (1965). Changes in the enzyme activities of *Saccharomyces cerevisiae* during aerobic growth on different carbon sources. *Biochem. J.* **97**, 284–297.
- Qi, K., Zhong, J.-J., and Xia, X.-X. (2014). Triggering respirofermentative metabolism in the crabtree-negative yeast *Pichia guilliermondii* by disrupting the CAT8 gene. *Appl. Environ. Microbiol.* **80**, 3879–3887.
- Rhee, H.S., and Pugh, B.F. (2012). Genome-wide structure and organization of eukaryotic pre-initiation complexes. *Nature* **483**, 295–301.
- Santangelo, G.M. (2006). Glucose signaling in *Saccharomyces cerevisiae*. *Microbiol. Mol. Biol. Rev.* **70**, 253–282.
- Service, R.F. (2014). Renewable energy. Cellulosic ethanol at last? *Science* **345**, 1111.
- Tachibana, C., Yoo, J.Y., Tagne, J.B., Kacherovsky, N., Lee, T.I., and Young, E.T. (2005). Combined global localization analysis and transcriptome data identify genes that are directly coregulated by Adr1 and Cat8. *Mol. Cell. Biol.* **25**, 2138–2146.
- Tamari, Z., Rosin, D., Voicheck, Y., and Barkai, N. (2014). Coordination of gene expression and growth-rate in natural populations of budding yeast. *PLoS ONE* **9**, e88801.
- Venters, B.J., Wachi, S., Mavrich, T.N., Andersen, B.E., Jena, P., Sinnamon, A.J., Jain, P., Rolleri, N.S., Jiang, C., Hemeryck-Walsh, C., and Pugh, B.F. (2011). A comprehensive genomic binding map of gene and chromatin regulatory proteins in *Saccharomyces*. *Mol. Cell* **41**, 480–492.
- Vidal, M., and Gaber, R.F. (1991). RPD3 encodes a second factor required to achieve maximum positive and negative transcriptional states in *Saccharomyces cerevisiae*. *Mol. Cell. Biol.* **11**, 6317–6327.
- Vidal, M., Strich, R., Esposito, R.E., and Gaber, R.F. (1991). RPD1 (SIN3/UME4) is required for maximal activation and repression of diverse yeast genes. *Mol. Cell. Biol.* **11**, 6306–6316.
- Watanabe, D., Hashimoto, N., Mizuno, M., Zhou, Y., Akao, T., and Shimoi, H. (2013). Accelerated alcoholic fermentation caused by defective gene expression related to glucose derepression in *Saccharomyces cerevisiae*. *Biosci. Biotechnol. Biochem.* **77**, 2255–2262.
- Weinberger, L., Voicheck, Y., Tirosh, I., Hornung, G., Amit, I., and Barkai, N. (2012). Expression noise and acetylation profiles distinguish HDAC functions. *Mol. Cell* **47**, 193–202.
- Young, E.T., Dombek, K.M., Tachibana, C., and Ideker, T. (2003). Multiple pathways are co-regulated by the protein kinase Snf1 and the transcription factors Adr1 and Cat8. *J. Biol. Chem.* **278**, 26146–26158.
- Zaman, S., Lippman, S.I., Zhao, X., and Broach, J.R. (2008). How *Saccharomyces* responds to nutrients. *Annu. Rev. Genet.* **42**, 27–81.
- Zaman, S., Lippman, S.I., Schnepfer, L., Slonim, N., and Broach, J.R. (2009). Glucose regulates transcription in yeast through a network of signaling pathways. *Mol. Syst. Biol.* **5**, 245.